mathematics

MDPI

Article

Four-Quadrant Riemann Problem for a 2 × 2 System Involving Delta Shock

Jinah Hwang [1], Suyeon Shin [1], Myoungin Shin [2] and Woonjae Hwang [1,*]

[1] Division of Applied Mathematical Sciences, Korea University, Sejong 30019, Korea; jinahwang@korea.ac.kr (J.H.); angelic52@korea.ac.kr (S.S.)
[2] Department of Ocean Systems Engineering, Sejong University, Seoul 05006, Korea; Myoungin@sju.ac.kr
* Correspondence: woonjae@korea.ac.kr

Abstract: In this paper, a four-quadrant Riemann problem for a 2 × 2 system of hyperbolic conservation laws is considered in the case of delta shock appearing at the initial discontinuity. We also remove the restriction in that there is only one planar wave at each initial discontinuity. We include the existence of two elementary waves at each initial discontinuity and classify 14 topologically distinct solutions. For each case, we construct an analytic solution and compute the numerical solution.

Keywords: conservation laws; delta shock; 2-D Riemann problem

check for updates

Citation: Hwang, J.; Shin, S.; Shin, M.; Hwang, W. Four-Quadrant Riemann Problem for a 2 × 2 System Involving Delta Shock. *Mathematics* **2021**, *9*, 138. https://doi.org/10.3390/math9020138

Received: 11 December 2020
Accepted: 7 January 2021
Published: 10 January 2021

Publisher's Note: MDPI stays neutral with regard to jurisdictional claims in published maps and institutional affiliations.

Copyright: © 2021 by the authors. Licensee MDPI, Basel, Switzerland. This article is an open access article distributed under the terms and conditions of the Creative Commons Attribution (CC BY) license (https://creativecommons.org/licenses/by/4.0/).

1. Introduction

In 1977, in doctoral dissertation (thesis advisor, H. Kranzer), Korchinski [1] considered the Riemann problem (RP) for the system:

$$\begin{cases} u_t + (\frac{1}{2}u^2)_x = 0, \\ v_t + (\frac{1}{2}uv)_x = 0. \end{cases} \tag{1}$$

They found that the delta function is supported on a discontinuity, which was motivated by some numerical calculations of the Lax-Friedrich scheme, which was later called a delta shock.

For a hyperbolic system of conservation laws, the four-quadrant RP is the initial value problem:

$$U_t + f(U)_x + g(U)_y = 0 \tag{2}$$

with the initial data $U(x, y, 0) = U_i,\ i = 1, \cdots, 4$, where i denotes the ith quadrant. Here, $U(x, y, t) = \left(u_1(x, y, t), \cdots, u_n(x, y, t)\right)^T$ denotes an n-dimensional vector of conserved quantities, and f and g are nonlinear fluxes.

Since Zhang and Zheng's illuminating conjecture [2] on the classification and structure of the solution of four-quadrant RP for 2-D gas dynamics systems in 1990, many studies have been conducted on simplified gas-dynamics-like models.

In 1994, Tan and Zhang [3,4] studied a four-quadrant RP for a 2-D system:

$$\begin{cases} u_t + (u^2)_x + (uv)_y = 0, \\ v_t + (uv)_x + (v^2)_y = 0. \end{cases} \tag{3}$$

In a series of papers, they classified and constructed an analytic solution in the case of initial data involving four contact discontinuities $(4J)$ [3] and in the case of the initial data involving rarefaction waves [4]. They found the delta shock in this model independently of Korchinski, and Tan et al. [5] established the concept of a delta shock. In addition, Pang et al. [6,7], and Shen [8] considered three constant initial data for the system (3).

Under the assumption that $\rho = const. \equiv 1$, Zhang et al. [9] considered a four-quadrant RP for pressure-gradient equations (4) of the compressible Euler system:

$$\begin{cases} u_t + p_x = 0, \\ v_t + p_y = 0, \\ E_t + (pu)_x + (pv)_y = 0, \end{cases} \tag{4}$$

where p is the pressure, (u, v) is the velocity, and $E = (u^2 + v^2)/2 + p$ is the energy. Shen and Sun [10] considered the system (4) with the initial data of three constants in three fan domains.

Sheng and Zhang [11] solved a four-quadrant RP for a 2-D system, which is called the transportation equation:

$$\begin{cases} \rho_t + (\rho u)_x + (\rho v)_y = 0, \\ (\rho u)_t + (\rho u^2)_x + (\rho uv)_y = 0, \\ (\rho v)_t + (\rho uv)_x + (\rho v^2)_y = 0. \end{cases} \tag{5}$$

Cheng et al. [12] considered the RP for the zero-pressure gas dynamics model (5) with three constant states, and Mach reflection-like configurations appear in some of the solutions.

The 2-D RP for Chaplygin gas dynamics with three and four constant states were investigated by Wang et al. [13] and Chen and Qu [14], respectively. Shearer [15] studied the RP for 2×2 systems of nonstrictly hyperbolic conservation laws with quadratic nonlinearities that are nondegenerate. In addition, Andrianov and Warnecke [16] considered the RP for compressible duct flows.

Most of the RPs cited above were applied under the following assumption [17]:

> (H) *Outside a neighborhood of the origin, each jump of the initial data projects exactly one plane elementary wave.*

This is a restricted assumption for systems because an $n \times n$ system can generally develop n waves at each initial discontinuity. Most of the RPs citations below were done without the above assumption (H).

In a series of papers [18,19], Hwang and Lindquist solved the 2-D RP of the system (6), which is a generalization of the 1-D Keyfitz–Kranzer–Issacson–Temple model [20–22]:

$$\begin{cases} s_t + f^A(s,c)_x + f^B(s,c)_y = 0, \\ (cs)_t + (cf^A(s,c))_x + (cf^B(s,c))_y = 0, \end{cases} \tag{6}$$

where

$$f^k(s,c) = s^2[1 + k(1-c)(1-s)], \quad 0 < k < \frac{1}{2}, \text{ for } k = A, B. \tag{7}$$

Under the fundamental assumption of $u = v$, Sun [23] constructed six topologically distinct solutions for a nonstrictly hyperbolic system (8) :

$$\begin{cases} \rho_t + (\rho u)_x + (\rho u)_y = 0, \\ u_t + (\frac{u^2}{2})_x + (\frac{u^2}{2})_y = 0. \end{cases} \tag{8}$$

Shen et al. [24] constructed ten solutions for the system (9):

$$\begin{cases} u_t + (u^2)_x + (u^2)_y = 0, \\ \rho_t + (\rho u)_x + (\rho u)_y = 0. \end{cases} \tag{9}$$

This equation can also be considered to be a simplified gas-dynamics-like model because it can be derived from 2-D isentropic Euler equations [25]. Because this is an isotropic case ($f = g$ in Equation (2)), they considered interactions in the $\eta > \xi$ plane by applying the

transformation and symmetry. Hwang et al. [26] considered a 2-D RP with three constant initial data for the system (9). They classified and constructed 12 solutions.

In this paper, our interest is to classify and construct the analytic solution for a 2×2 hyperbolic system (9) in the case of initial four-quadrant data without the assumption (H). We consider Riemann's initial data involving delta shock. The numerical solution is also computed for comparison with the analytical solution.

We apply the 2-D direct construction method within the entire plane. This approach has certain advantages because the wave interactions in the full plane can be seen, and the constructed analytic solutions can be compared with numerical solutions. The results show extremely interesting structures of wave interactions of the RP, and the numerical solution is remarkably coincident with the constructed analytic solution. Because the theory gives little insight for the qualitative behavior of wave interactions, we need to construct the solution for each system. Furthermore, since general theory does not exist for multidimensional system, 2-D RP for systems must be investigated on a case-by-case basis.

In Section 2, preliminaries, including elementary waves, are presented. In Section 3, the initial data involving the delta shock are formally classified as 52 cases, which results in 14 solutions. We construct analytic and numerical solutions for each case.

2. Preliminaries

The system (9) is changed to a self-similar form

$$\begin{cases} -\xi u_\xi - \eta u_\eta + (u^2)_\xi + (u^2)_\eta = 0, \\ -\xi \rho_\xi - \eta \rho_\eta + (\rho u)_\xi + (\rho u)_\eta = 0, \end{cases} \tag{10}$$

through $\xi = x/t$, $\eta = y/t$. The system (10) has two eigenvalues and the corresponding right eigenvectors:

$$\lambda_1 = \frac{u-\eta}{u-\xi}, \quad \lambda_2 = \frac{2u-\eta}{2u-\xi}, \; r_1 = (0,1)^T, \; r_2 = (u,\rho)^T. \tag{11}$$

Then, the λ_1 field is linearly degenerated and the λ_2 field is genuinely nonlinear if $\eta \neq \xi$ and $u \neq 0$.

From the initial discontinuity between two sides (u_l, ρ_l) and (u_r, ρ_r) in the counterclockwise direction, we use the notation R_{lr}, J_{lr}, S_{lr}, $S_{\delta_{lr}}$ for the rarefaction wave, contact discontinuity, shock, and delta shock, respectively.

From the Rankine–Hugoniot condition, the contact discontinuity satisfies

$$\frac{d\eta}{d\xi} = \frac{\eta - u_l}{\xi - u_l} = \frac{\eta - u_r}{\xi - u_r}, \tag{12}$$

which shows that it is directed to the singular point $(u_l, u_l) = (u_r, u_r)$. Here, $J_{lr}(\xi)$ can be expressed as

$$J_{lr}(\xi) \; : \; \xi = u_l = u_r. \tag{13}$$

Again, from the jump condition, the shock satisfies

$$\frac{d\eta}{d\xi} = \frac{\eta - (u_l + u_r)}{\xi - (u_l + u_r)}, \; \frac{\rho_l}{u_l} = \frac{\rho_r}{u_r}, \tag{14}$$

which shows that it directs to the singular point $(u_l + u_r, u_l + u_r)$. The entropy condition is defined as three characteristic "incoming" lines and the remaining "outgoing" line. The shock $S_{lr}(\xi)$ can be expressed as follows:

$$\begin{gathered} S_{lr}(\xi) \; : \; \xi = u_l + u_r, \quad \frac{\rho_l}{u_l} = \frac{\rho_r}{u_r}, \\ \big(0 < u_l < u_r \text{ or } u_l < u_r < 0 \text{ for } \eta > \xi, \; 0 < u_r < u_l \text{ or } u_r < u_l < 0 \text{ for } \eta < \xi\big). \end{gathered} \tag{15}$$

Again, from the generalized Rankine–Hugoniot condition, the delta shock is directed to the singular point $(u_l + u_r, u_l + u_r)$. The entropy condition of delta shock implies that all characteristics on both sides of the delta shock are "non-outgoing" [24]. The delta shock $S_{\delta_{lr}}(\xi)$ can be expressed as follows:

$$S_{\delta_{lr}}(\xi) \ : \ \xi = u_l + u_r, \quad (u_l < 0 < u_r \text{ for } \eta > \xi, \ u_r < 0 < u_l \text{ for } \eta < \xi). \tag{16}$$

The delta shock is described in detail in [3,5,24,27,28].

However, because the second characteristic line satisfies

$$\frac{d\eta}{d\xi} = \frac{\eta - 2u}{\xi - 2u} \tag{17}$$

which shows that it directs $(2u, 2u)$, $R_{lr}(\xi)$ can be expressed as follows:

$$R_{lr}(\xi) \ : \ \xi = 2u, \quad \frac{\rho}{u} = \frac{\rho_l}{u_l}, \ (u_r \le u \le u_l \text{ for } \eta > \xi, \ u_l \le u \le u_r \text{ for } \eta < \xi). \tag{18}$$

Here, (13), (15), (16), and (18) represent the waves that are parallel to the η-axis. The waves parallel to the ξ-axis can be described in a similar manner.

3. Construction of the Solution

We consider a four-quadrant RP for system (9). From the entropy condition, all four characteristics are incoming from both sides of the delta shock. This means that 0 is between the two states. Thus, we must consider the order of u_1, u_2, u_3, u_4, and 0 because of delta shock, which brings a total of 5! = 120 cases. The cases including a delta shock are reduced to 52 cases, which resulted in 14 topologically distinct solutions.

Because we remove the assumption (H), there is one or two waves at infinity for each discontinuity. Consider the values of u on either side of the initial discontinuity. If they have the same sign, then we have two waves: a contact shock (JS) or contact rarefaction (JR). If they have different signs, then we have only one wave: S_δ or R.

Because one of the fields of the system (9) is linearly degenerate, contact discontinuity appears as a solution of the RP. For the numerical solution, to reduce the numerical dissipations of the contact discontinuity, the flux functions of the semi-discrete central upwind scheme are modified. Further details can be found in [26,29,30]. In this study, the computational domain is $[-4, 4] \times [-4, 4]$ and t = 0.2, $\rho_i = 0.77$ for $i = 1, \cdots, 4$. We use 1200×1200 cells, and the CFL is 0.05.

3.1. Two Delta Shocks

For the classification of waves at the initial discontinuities, we count the exterior waves that come from the positive η-axis at first, and then at the axes in the counterclockwise direction. In the classification of the initial data, 21034 and 41032 indicate that $u_2 < u_1 < 0 < u_3 < u_4$ and $u_4 < u_1 < 0 < u_3 < u_2$, respectively.

3.1.1. No Shock Wave

The upper and lower sides of the line $\eta = \xi$ form a symmetrical structure in each of the following cases

$$\begin{array}{ll}
\text{Case 1}: & JR + S_\delta + JR + S_\delta \ (21034), \ S_\delta + RJ + S_\delta + RJ \ (41032) \\
\text{Case 2}: & JR + S_\delta + S_\delta + RJ(24103, 42103), S_\delta + RJ + JR + S_\delta(10324, 10342) \\
\text{Case 3}: & S_\delta + R + R + S_\delta \ (31024, \ 31042), R + S_\delta + S_\delta + R \ (24031, \ 42031) \\
\text{Case 4}: & S_\delta + R + R + S_\delta \ (13024, \ 13042), R + S_\delta + S_\delta + R \ (24013, \ 42013)
\end{array}$$

Case 1. $JR + S_\delta + JR + S_\delta \ \ (u_2 < u_1 < 0 < u_3 < u_4)$

From the initial discontinuity at the positive η-axis, the contact J_{1a} and the rarefaction R_{a2} are developed, and a new state (u_a, ρ_a) satisfies $u_a = u_1$ and $\frac{\rho_a}{u_a} = \frac{\rho_2}{u_2}$. Here, J_{1a} is

directed to the singular point (u_1, u_1), and the rarefaction R_{a2} is directed to the singular point $(2u, 2u)$ for $u_2 \leq u \leq u_1$. From the initial discontinuity at the negative ξ-axis, the exterior wave connecting states (u_2, ρ_2) and (u_3, ρ_3) is $S_{\delta_{23}}$ parallel to the negative ξ-axis. In addition, $S_{\delta_{23}}$ is directed to the singular point $(u_2 + u_3, u_2 + u_3)$. From the initial discontinuity at the negative η-axis, J_{3c} and R_{c4} are developed, and a new state (u_c, ρ_c) satisfies $u_c = u_3$ and $\frac{\rho_c}{u_c} = \frac{\rho_4}{u_4}$. Moreover, J_{3c} is directed to the singular point (u_3, u_3), and the rarefaction R_{c4} is directed to $(2u, 2u)$ for $u_3 \leq u \leq u_4$. From the initial discontinuity at the positive ξ-axis, the exterior wave connecting states (u_4, ρ_4) and (u_1, ρ_1) is $S_{\delta_{41}}$ parallel to the positive ξ-axis. Finally, $S_{\delta_{41}}$ is directed to the singular point $(u_4 + u_1, u_4 + u_1)$.

The straight delta shock $S_{\delta_{23}}$ completely penetrates the rarefaction wave R_{a2} at point $A(2u_2, u_1 + u_2)$, and then the curved delta shock $\eta = \eta(\xi)$ from A to $B(2u_1, \frac{u_1^2+u_3^2-2u_1u_2}{u_3-u_2})$ satisfies

$$\frac{d\eta}{d\xi} = \frac{\eta - (u + u_3)}{\xi - (u + u_3)}, \ \xi = 2u, \ \frac{\rho}{u} = \frac{\rho_2}{u_2}, \ u_2 \leq u \leq u_1, \tag{19}$$

and we obtain

$$\eta = \xi + \frac{1}{u_3 - u_2}\left(\frac{\xi}{2} - u_3\right)^2, \ 2u_2 \leq \xi \leq 2u_1. \tag{20}$$

This straight delta shock $S_{\delta_{a3}}$ meets the contact discontinuity J_{1a} at point $C(u_1, \frac{u_3^2-u_1u_2}{u_3-u_2})$ and continues to the singular point $D(u_1 + u_3, u_1 + u_3)$, and has the form

$$\eta - (u_1 + u_3) = \frac{u_1 - u_2}{u_3 - u_2}(\xi - (u_1 + u_3)), \ 2u_1 \leq \xi \leq u_1 + u_3. \tag{21}$$

By contrast, the delta shock $S_{\delta_{41}}$ penetrates the whole rarefaction wave R_{c4}, and the straight delta shock $S_{\delta_{c1}}$ from the point $E(2u_3, \frac{u_1^2+u_3^2-2u_3u_4}{u_1-u_4})$ then meets J_{3c} at the point $F(u_3, \frac{u_1^2-u_3u_4}{u_1-u_4})$ and continues to the singular point D. The solutions are provided in Figure 1 and show good agreement. The initial condition is $u_1 = -0.15$, $u_2 = -0.37$, $u_3 = 0.43$, $u_4 = 0.56$.

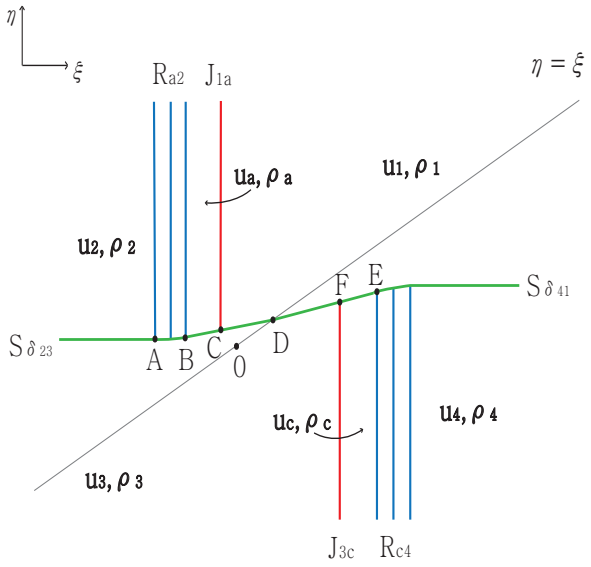

(**a**) Analytical solution

Figure 1. *Cont.*

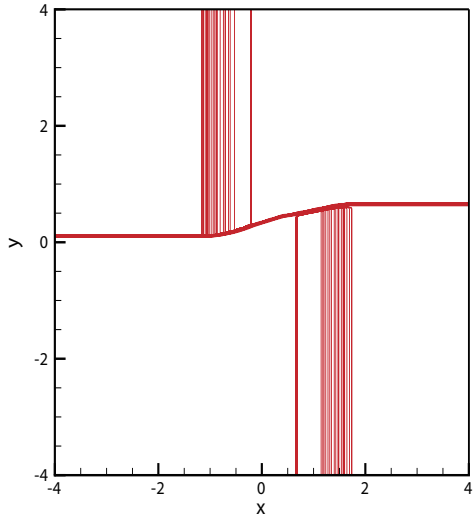

(**b**) Numerical solution

Figure 1. Case 1. $JR + S_\delta + JR + S_\delta$.

Case 2. $JR + S_\delta + S_\delta + RJ \ \ (u_2 < u_4 < u_1 < 0 < u_3)$

From the initial discontinuity, a delta shock is formed at the negative ξ-axis and negative η-axis, and contact rarefaction is formed at the positive η-axis and positive ξ-axis. The delta shock $S_{\delta_{23}}$ penetrates the entire rarefaction wave R_{a2}. The straight delta shock $S_{\delta_{a3}}$ from point $A(2u_1, \frac{u_1^2+u_3^2-2u_1u_2}{u_3-u_2})$ meets the contact discontinuity J_{1a} at point $C(u_1, \frac{u_1u_2-u_3^2}{u_2-u_3})$ and continues to the singular point $B(u_1+u_3, u_1+u_3)$.

By contrast, the delta shock $S_{\delta_{34}}$ completely penetrates the rarefaction wave R_{4d}. The straight delta shock $S_{\delta_{3d}}$ from the point $D(\frac{u_1^2+u_3^2-2u_1u_4}{u_3-u_4}, 2u_1)$ meets the contact discontinuity J_{d1} at point $E(\frac{u_1u_4-u_3^2}{u_4-u_3}, u_1)$, and then continues to the singular point $B(u_1+u_3, u_1+u_3)$. The solutions are shown in Figure 2. The initial condition for the numerical computation is $u_1 = -0.37$, $u_2 = -0.56$, $u_3 = 0.15$, $u_4 = -0.43$.

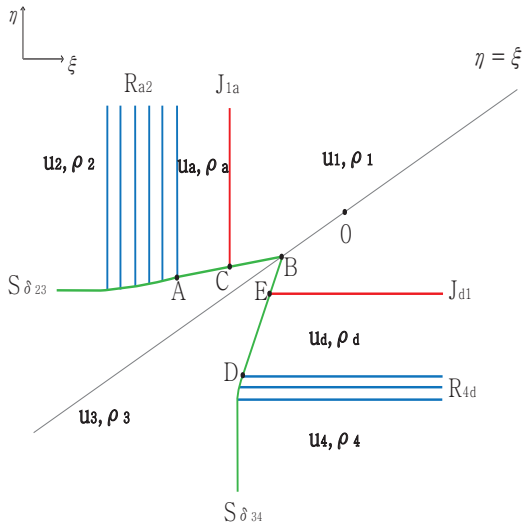

(**a**) Analytical solution

Figure 2. *Cont.*

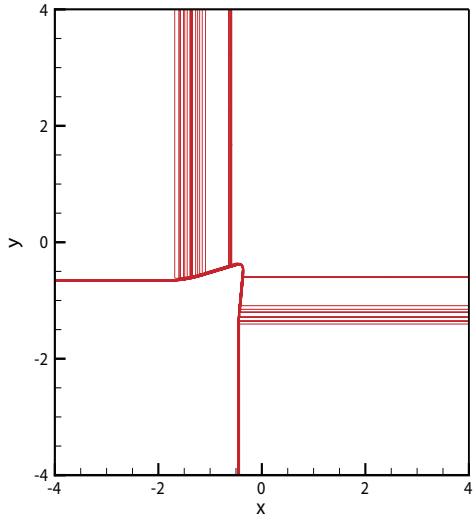

(**b**) Numerical solution

Figure 2. Case 2. $JR + S_\delta + S_\delta + RJ$.

Case 3. $R + S_\delta + S_\delta + R \ \ (u_2 < u_4 < 0 < u_3 < u_1)$

In this case, only one wave is formed at each initial discontinuity. From the initial discontinuity at the positive η-axis, the exterior wave connecting states (u_1, ρ_1) and (u_2, ρ_2) is the rarefaction R_{12} parallel to the positive η-axis. The rarefaction R_{12} is directed to $(2u, 2u)$ for $u_2 \le u \le u_1$. From the initial discontinuity at the negative ξ-axis, the exterior wave connecting states (u_2, ρ_2) and (u_3, ρ_3) is $S_{\delta_{23}}$, which is directed to the singular point $(u_2 + u_3, u_2 + u_3)$. From the initial discontinuity at the negative η-axis, the exterior wave connecting states (u_3, ρ_3) and (u_4, ρ_4) is $S_{\delta 34}$, which is directed to the singular point $(u_3 + u_4, u_3 + u_4)$. From the initial discontinuity at the positive ξ-axis, the exterior wave connecting states (u_4, ρ_4) and (u_1, ρ_1) is the rarefaction R_{41}, which is directed to $(2u, 2u)$ for $u_4 \le u \le u_1$.

The straight delta shock $S_{\delta_{23}}$ meets the rarefaction wave R_{a2} at point $A(2u_2, u_1 + u_2)$, and the curved delta shock $\eta = \eta(\xi)$ from A to $B(0, \frac{u_3^2}{u_3 - u_2})$ then satisfies

$$\frac{d\eta}{d\xi} = \frac{\eta - (u + u_3)}{\xi - (u + u_3)}, \ \xi = 2u, \ \frac{\rho}{u} = \frac{\rho_2}{u_2}, \ u_2 \le u \le 0, \tag{22}$$

and we obtain

$$\eta = \xi + \frac{1}{u_3 - u_2}\left(\frac{\xi}{2} - u_3\right)^2, \ 2u_2 \le \xi \le 0. \tag{23}$$

Simultaneously, a new shock and a new contact discontinuity occur at B. This is an extremely interesting phenomenon in which the delta shock is switched into shock and contact discontinuity. This new shock satisfies the equations in (22) in $0 \le u \le u_3$. Similarly, this curved shock has the same form as (23), and continues to $C(2u_3, 2u_3)$. In addition, J_{e3} formed at point B ends at the singular point $D(u_3, u_3)$ and satisfies

$$\eta - u_3 = \frac{u_2}{u_2 - u_3}(\xi - u_3), \quad 0 \le \xi \le u_3. \tag{24}$$

By contrast, $S_{\delta_{34}}$ meets R_{41} at the point $E(u_3 + u_4, 2u_4)$. The curved delta shock continues to point $F(\frac{u_3^2}{u_3 - u_4}, 0)$, and J_{3e} and S_{eu} $(0 \le u \le u_3)$ are formed at F. This shock continues to point C, and J_{3e} ends at the singular point D. This contact discontinuity J_{3e} meets the contact discontinuity J_{e3} at point D. Both rarefaction waves R_{12} and R_{41} meet at

the same singular point $(2u, 2u)$ for $u_3 \leq u \leq u_1$ between C and $G(2u_1, 2u_1)$. The solutions are shown in Figure 3. The initial condition is $u_1 = 0.56$, $u_2 = -0.37, u_3 = 0.43, u_4 = -0.15$.

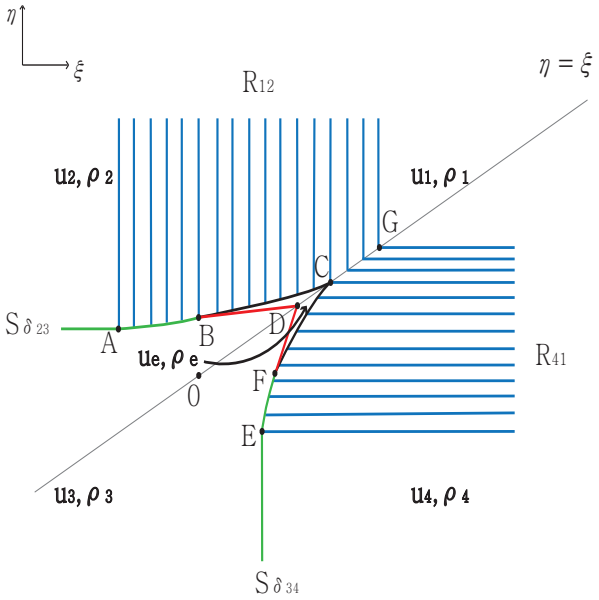

(**a**) Analytical solution

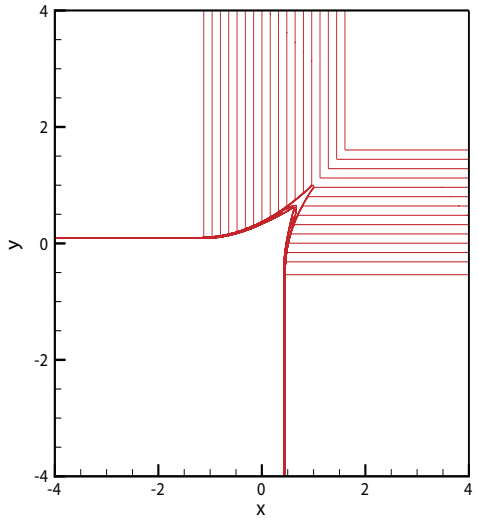

(**b**) Numerical solution

Figure 3. Case 3. $R + S_\delta + S_\delta + R$.

Case 4. $S_\delta + R + R + S_\delta \ \ (u_1 < u_3 < 0 < u_4 < u_2)$

As in case 3, only one wave, either a delta shock or rarefaction, is formed at each initial discontinuity. The straight delta shock $S_{\delta_{12}}$ meets the rarefaction wave R_{23} at point $A(u_1 + u_2, 2u_2)$. The curved delta shock continues from A to $B(\frac{u_1^2}{u_1 - u_2}, 0)$. Simultaneously, a new shock and a new contact discontinuity occur at B. This shock formed at point B completely penetrates the rarefaction wave R_{23} from B to $C(\frac{u_1^2 + u_3^2 - 2u_2u_3}{u_1 - u_2}, 2u_3)$, and ends at the singular point $D(u_1 + u_3, u_1 + u_3)$. Here, J_{1e} formed at point B ends at the singular point $E(u_1, u_1)$.

By contrast, $S_{\delta_{41}}$ meets R_{34} at the point $F(2u_4, u_4 + u_1)$. The curved delta shock continues to point $G(0, \frac{u_1^2}{u_1 - u_4})$, and J_{e1} and S_{ue} $(u_3 \leq u \leq 0)$ are formed at G. This shock formed

at point G completely penetrates the rarefaction wave R_{34} from G to $H(2u_3, \frac{u_1^2+u_3^2-2u_3u_4}{u_1-u_4})$ and ends at the singular point D. In addition, J_{e1} formed at point G ends at the singular point $E(u_1, u_1)$. The solutions are shown in Figure 4. The initial condition is $u_1 = -0.37$, $u_2 = 0.56$, $u_3 = -0.15$, $u_4 = 0.43$.

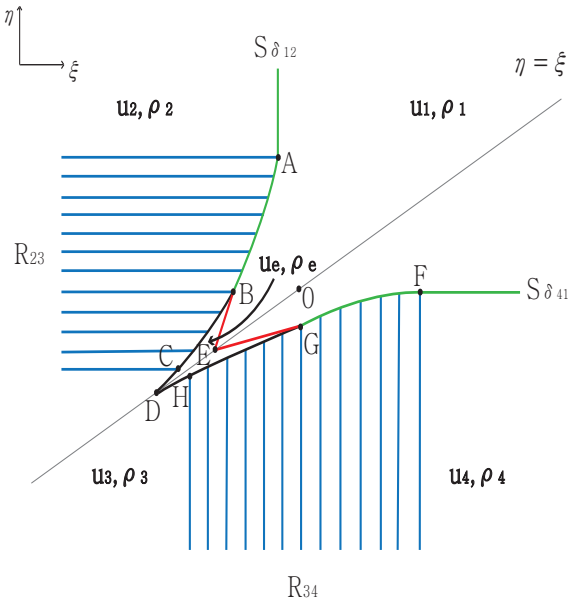

(**a**) Analytical solution

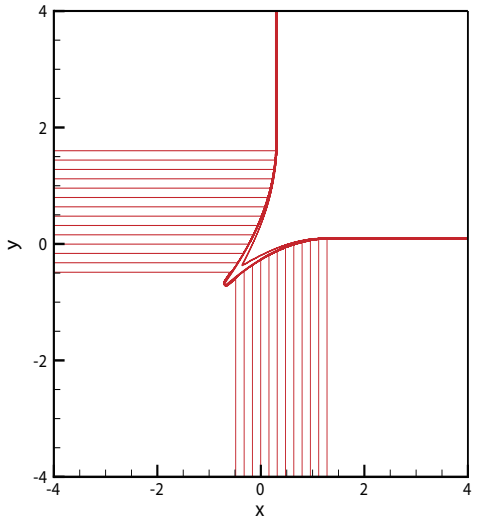

(**b**) Numerical solution

Figure 4. Case 4. $S_\delta + R + R + S_\delta$.

3.1.2. One Shock Wave

$$\text{Case 5}: \begin{cases} JS + S_\delta + JR + S_\delta \ (12034), \ S_\delta + RJ + S_\delta + SJ \ (14032) \\ JR + S_\delta + JS + S_\delta \ (21043), \ S_\delta + SJ + S_\delta + RJ \ (41023) \end{cases}$$

$$\text{Case 6}: \begin{cases} JR + S_\delta + S_\delta + SJ \ (21403), \ JS + S_\delta + S_\delta + RJ \ (41203) \\ S_\delta + SJ + JR + S_\delta \ (10234), \ S_\delta + RJ + JS + S_\delta \ (10432) \end{cases}$$

Case 5. $S_\delta + RJ + S_\delta + SJ \ \ (u_1 < u_4 < 0 < u_3 < u_2)$

From the initial discontinuity, a delta shock is formed at the positive η-axis and negative η-axis, and the rarefaction-contact and shock-contact are formed at the negative η-axis and positive ξ-axis, respectively. The delta shock $S_{\delta_{12}}$ completely penetrates the

rarefaction wave R_{2b}. The straight delta shock $S_{\delta_{1b}}$ from the point $A(\frac{u_1^2+u_3^2-2u_2u_3}{u_1-u_2}, 2u_3)$ meets the contact discontinuity J_{b3} at point $C(\frac{u_2u_3-u_1^2}{u_2-u_1}, u_3)$, and then continues to the singular point $B(u_1+u_3, u_1+u_3)$.

By contrast, the delta shock $S_{\delta_{34}}$ intersects with the shock S_{4d} at point $D(u_3+u_4, u_4+u_1)$. Then, the new delta shock $S_{\delta_{3d}}$ from D to B satisfies

$$\eta-(u_1+u_3)=\frac{u_3-u_4}{u_1-u_4}(\xi-(u_1+u_3)),\ u_1+u_3\le\xi\le u_3+u_4. \tag{25}$$

The straight delta shock $S_{\delta_{3d}}$ meets the contact discontinuity J_{d1} at point $E(\frac{u_1u_4-u_3^2}{u_4-u_3}, u_1)$ and continues to the singular point B. The solutions are shown in Figure 5. The initial condition is $u_1=-0.37$, $u_2=0.56$, $u_3=0.43$, $u_4=-0.15$.

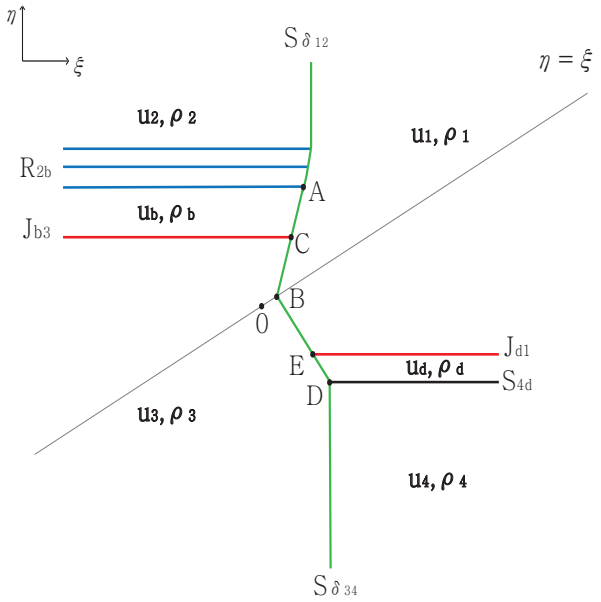

(**a**) Analytical solution

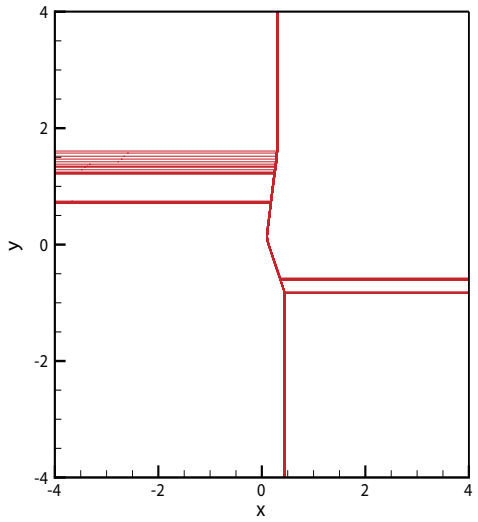

(**b**) Numerical solution

Figure 5. Case 5. $S_\delta+RJ+S_\delta+SJ$.

Case 6. $JS + S_\delta + S_\delta + RJ \ \ (u_4 < u_1 < u_2 < 0 < u_3)$

From the initial discontinuity, a delta shock is formed at the negative ξ-axis and negative η-axis, and contact shock and contact rarefaction contact are formed at the positive η-axis and positive ξ-axis, respectively. The delta shock $S_{\delta_{23}}$ meets the shock S_{a2} at point $A(u_1 + u_2, u_2 + u_3)$. The new delta shock $S_{\delta_{a3}}$ formed at A meets the contact discontinuity J_{1a} at $C(u_1, \frac{u_1u_2-u_3^2}{u_2-u_3})$ and continues to the singular point $B(u_1 + u_3, u_1 + u_3)$.

By contrast, the delta shock $S_{\delta_{34}}$ penetrates the entire rarefaction wave R_{4d}, and the straight delta shock $S_{\delta_{3d}}$ from the point $D(\frac{u_1^2+u_3^2-2u_1u_4}{u_3-u_4}, 2u_1)$ then meets the contact discontinuity J_{d1} at the point $E(\frac{u_1u_4-u_3^2}{u_4-u_3}, u_1)$ and continues to the singular point $B(u_1 + u_3, u_1 + u_3)$. The solutions are shown in Figure 6. The initial condition is $u_1 = -0.43$, $u_2 = -0.37$, $u_3 = 0.15$, $u_4 = -0.56$.

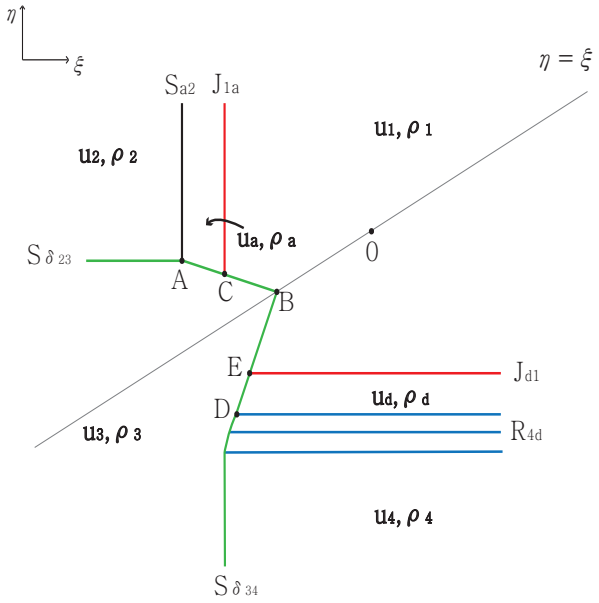

(**a**) Analytical solution

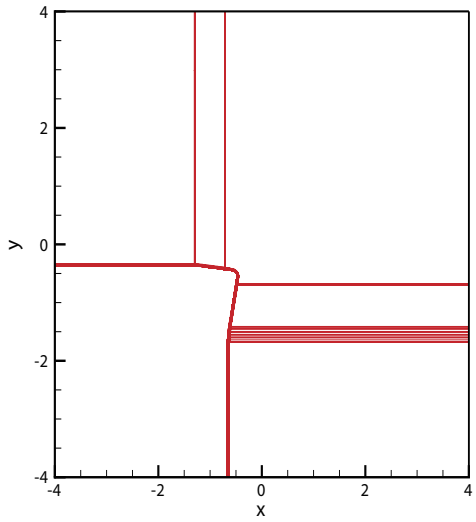

(**b**) Numerical solution

Figure 6. Case 6. $JS + S_\delta + S_\delta + RJ$.

3.1.3. Two Shock Waves

Case 7 : $JS + S_\delta + JS + S_\delta$ (12043), $S_\delta + SJ + S_\delta + SJ$ (14023)
Case 8 : $JS + S_\delta + S_\delta + SJ$ (12403, 14203), $S_\delta + SJ + JS + S_\delta$ (10243, 10423)

Case 7. $JS + S_\delta + JS + S_\delta$ $(u_1 < u_2 < 0 < u_4 < u_3)$

From the initial discontinuity, a delta shock is formed at the negative ξ-axis and positive ξ-axis, and a contact shock is formed at the positive η-axis and negative η-axis. The delta shock $S_{\delta_{23}}$ meets the shock S_{a2} at point $A(u_1 + u_2, u_2 + u_3)$. The new delta shock $S_{\delta_{a3}}$ formed at A meets the contact discontinuity J_{1a} at $C(u_1, \frac{u_1 u_2 - u_3^2}{u_2 - u_3})$ and continues to the singular point $B(u_1 + u_3, u_1 + u_3)$ without changing the direction because $u_a = u_1$.

However, the delta shock $S_{\delta_{41}}$ intersects with the shock S_{c4} at the point $D(u_3 + u_4, u_4 + u_1)$. The new delta shock $S_{\delta_{c1}}$ formed at D meets the contact discontinuity J_{3c} at the point $E(u_3, \frac{u_3 u_4 - u_1^2}{u_4 - u_1})$ and continues to the singular point $B(u_1 + u_3, u_1 + u_3)$. The solutions are shown in Figure 7. The initial condition is $u_1 = -0.37$, $u_2 = -0.15$, $u_3 = 0.56$, $u_4 = 0.43$.

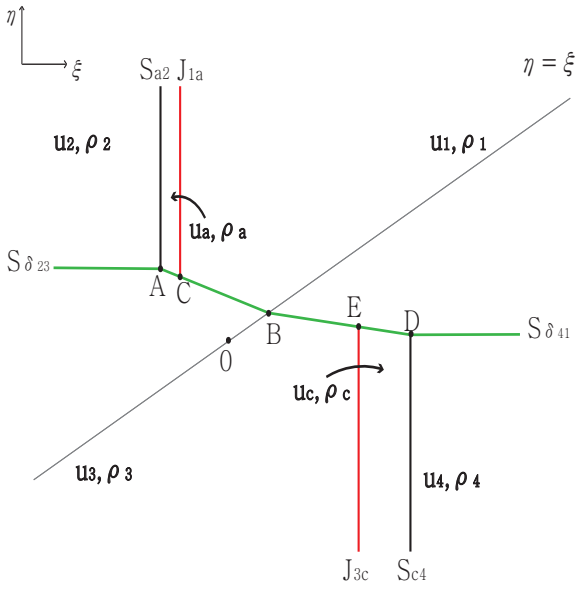

(**a**) Analytical solution

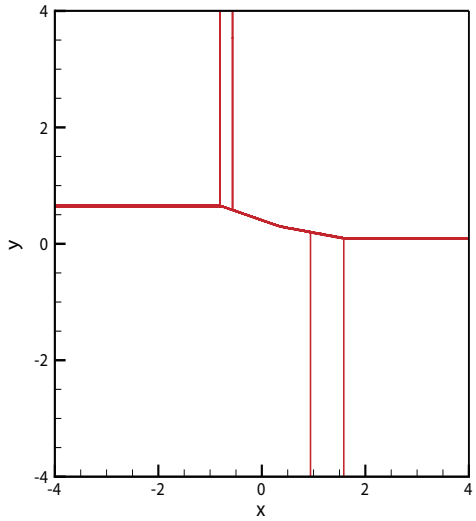

(**b**) Numerical solution

Figure 7. Case 7. $JS + S_\delta + JS + S_\delta$.

Case 8. $JS + S_\delta + S_\delta + SJ \ \ (u_1 < u_2 < u_4 < 0 < u_3)$

From the initial discontinuity, a delta shock is formed at the negative ξ-axis and negative η-axis, and a contact shock is formed at the positive η-axis and positive ξ-axis. The delta shock $S_{\delta_{23}}$ meets the shock S_{a2} at point $A(u_1 + u_2, u_2 + u_3)$. The new delta shock $S_{\delta_{a3}}$ formed at A meets the contact discontinuity J_{1a} at $C(u_1, \frac{u_1 u_2 - u_3^2}{u_2 - u_3})$ and continues to the singular point $B(u_1 + u_3, u_1 + u_3)$.

By contrast, the delta shock $S_{\delta_{34}}$ intersects with the shock S_{4d} at point $D(u_3 + u_4, u_4 + u_1)$. The new delta shock $S_{\delta_{3d}}$ formed at D meets the contact discontinuity J_{d1} at $E(u_3, \frac{u_3 u_4 - u_1^2}{u_4 - u_1})$ and continues to the singular point $B(u_1 + u_3, u_1 + u_3)$. The solutions are shown in Figure 8. The initial condition is $u_1 = -0.56$, $u_2 = -0.43$, $u_3 = 0.15$, $u_4 = -0.37$.

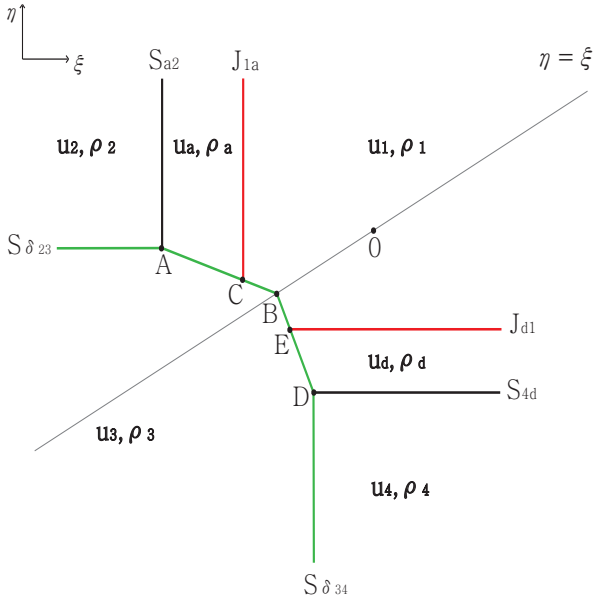

(**a**) Analytical solution

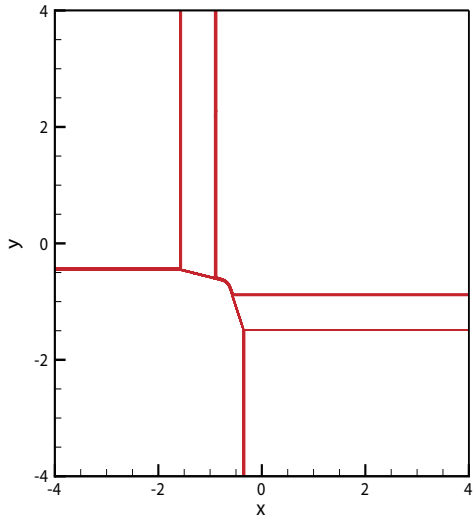

(**b**) Numerical solution

Figure 8. Case 8. $JS + S_\delta + S_\delta + SJ$.

3.2. One Delta Shock

3.2.1. No Shock Wave

$$\text{Case 9}: \begin{cases} JR + JR + R + S_\delta \ (32104), \ S_\delta + R + RJ + RJ \ (34102) \\ R + S_\delta + JR + JR \ (20341), \ RJ + RJ + S_\delta + R \ (40321) \end{cases}$$

Case 9. $R + S_\delta + JR + JR \ \ (u_2 < 0 < u_3 < u_4 < u_1)$

From the initial discontinuity at the positive η-axis, the exterior wave connecting states (u_1, ρ_1) and (u_2, ρ_2) is the rarefaction R_{12}. The rarefaction R_{12} is directed toward $(2u, 2u)$ for $u_2 \le u \le u_1$. From the initial discontinuity at the negative ξ-axis, the exterior wave connecting states (u_2, ρ_2) and (u_3, ρ_3) is the delta shock $S_{\delta_{23}}$. The delta shock $S_{\delta_{23}}$ is directed to the singular point $(u_2 + u_3, u_2 + u_3)$. From the initial discontinuity at the negative η-axis, the contact discontinuity J_{3c} and rarefaction R_{c4} and (u_c, ρ_c) between J_{3c} and R_{c4} satisfy $u_c = u_3$ and $\frac{\rho_c}{u_c} = \frac{\rho_4}{u_4}$. Here, J_{3c} is directed toward the singular point (u_3, u_3), and the rarefaction R_{c4} is directed toward $(2u, 2u)$ for $u_3 \le u \le u_4$. From the initial discontinuity at the positive ξ-axis, the contact discontinuity J_{4d} and the rarefaction R_{d1} and a new state (u_d, ρ_d) between J_{4d} and R_{d1} are formed. The state (u_d, ρ_d) satisfies $u_d = u_4$ and $\frac{\rho_d}{u_d} = \frac{\rho_1}{u_1}$. In addition, J_{4d} is directed toward the singular point (u_4, u_4), and the rarefaction R_{d1} is directed toward $(2u, 2u)$ for $u_4 \le u \le u_1$. The delta shock $S_{\delta_{23}}$ meets the rarefaction wave R_{12} at point $(2u_2, u_2 + u_3)$. Then, a curved delta shock continues toward point $A(0, \frac{u_3^2}{u_3 - u_2})$. Simultaneously, J_{e3} and S_{ue} $(0 \le u \le u_3)$ are formed at A. This curved shock continues toward point $B(2u_3, 2u_3)$, and J_{e3} ends at the singular point $C(u_3, u_3)$. By contrast, both R_{12} and R_{c4} meet at $(2u, 2u)$ for $u_3 \le u \le u_4$ between $B(2u_3, 2u_3)$ and $D(2u_4, 2u_4)$. In addition, J_{4d} penetrates the entire rarefaction wave, R_{c4}. The straight contact discontinuity continues from $(2u_3, \frac{2u_3u_4 - u_3^2}{u_4})$ toward $C(u_3, u_3)$. Consequently, three contact discontinuities J_{e3}, J_{3c}, and J_{ce} meet at their singular point C. Both rarefaction waves R_{12} and R_{d1}meet at $(2u, 2u)$ for $u_4 \le u \le u_1$ between D and $E(2u_1, 2u_1)$. The solutions are shown in Figure 9. The initial condition is $u_1 = 0.56$, $u_2 = -0.15$, $u_3 = 0.37$, $u_4 = 0.43$.

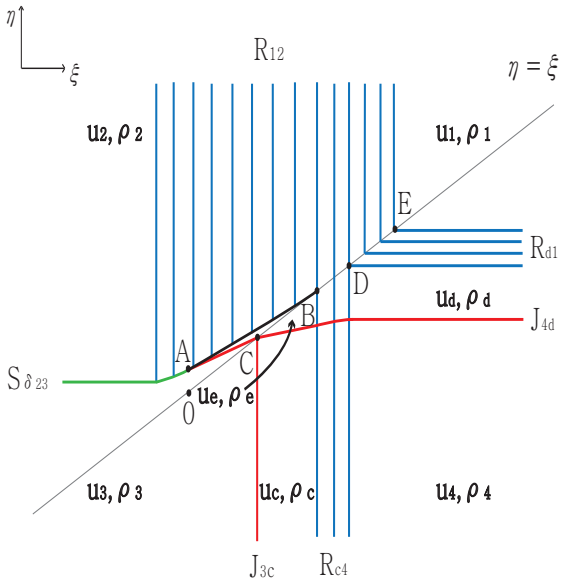

(**a**) Analytical solution

Figure 9. *Cont.*

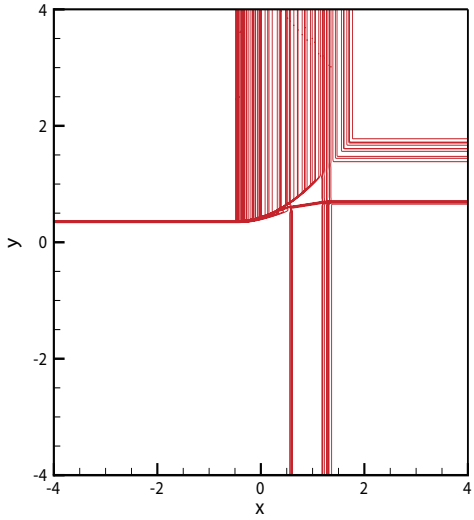

(**b**) Numerical solution

Figure 9. Case 9. $R + S_\delta + JR + JR$.

3.2.2. One Shock Wave

$$\text{Case 10}: \begin{cases} JS + JR + R + S_\delta\ (13204),\ S_\delta + R + RJ + SJ\ (13402) \\ R + S_\delta + JS + JR\ (20413),\ RJ + SJ + S_\delta + R\ (40213) \end{cases}$$

$$\text{Case 11}: \begin{cases} JS + JR + R + S_\delta\ (31204),\ S_\delta + R + RJ + SJ\ (31402) \\ R + S_\delta + JS + JR\ (20431),\ RJ + SJ + S_\delta + R\ (40231) \end{cases}$$

$$\text{Case 12}: \begin{cases} JR + JS + R + S_\delta\ (21304),\ S_\delta + R + SJ + RJ\ (41302) \\ R + S_\delta + JR + JS\ (20134),\ SJ + RJ + S_\delta + R\ (40132) \end{cases}$$

$$\text{Case 13}: \begin{cases} JR + JS + R + S_\delta\ (23104),\ S_\delta + R + SJ + RJ\ (43102) \\ R + S_\delta + JR + JS\ (20314),\ SJ + RJ + S_\delta + R\ (40312) \end{cases}$$

Case 10. $S_\delta + R + RJ + SJ\ \ (u_1 < u_3 < u_4 < 0 < u_2)$

From the initial discontinuity, a delta shock is formed at the positive η-axis, and a rarefaction is formed at the negative ξ-axis, and the rarefaction-contact and shock-contact are formed at the negative η-axis and positive ξ-axis, respectively. The delta shock $S_{\delta_{12}}$ meets the rarefaction wave R_{23} at point $A(u_1 + u_2, 2u_2)$. Then, the curved delta shock continues toward point $B(\frac{u_1^2}{u_1 - u_2}, 0)$. A new shock and a new contact discontinuity are formed at B, and this curved shock ends at point $C(\frac{u_1^2 + u_3^2 - 2u_2u_3}{u_1 - u_2}, 2u_3)$. Then, S_{e3} continues from point C to $D(u_1 + u_3, u_1 + u_3)$, and J_{1e} continues from point B to point $E(u_1, u_1)$. By contrast, J_{c4} intersects with S_{4d} at point $F(u_4, u_4 + u_1)$ and the new contact discontinuity J_{ed} from F ends at their singular point E, which equals the singular point of J_{d1} and J_{1e}. Therefore, the three contact discontinuities meet at the singular point E. The shock $S_{ce}(= S_{4d})$ completely penetrates R_{3c} and then stops at the singular point D. The solutions are shown in Figure 10. The initial condition is $u_1 = -0.73$, $u_2 = 0.15$, $u_3 = -0.56$, $u_4 = -0.25$.

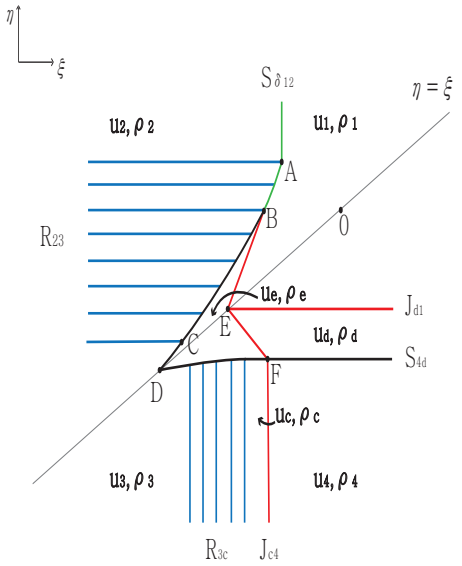

(**a**) Analytical solution

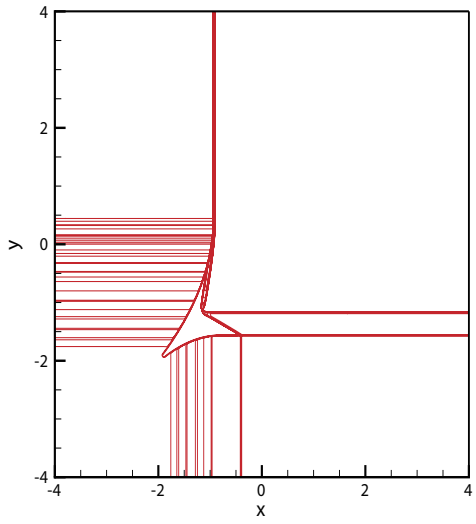

(**b**) Numerical solution

Figure 10. Case 10. $S_\delta + R + RJ + SJ$.

Case 11. $R + S_\delta + JS + JR \ \ (u_2 < 0 < u_4 < u_3 < u_1)$

From the initial discontinuity, rarefaction is formed at the positive η-axis, and a delta shock is formed at the negative ξ-axis, and contact shock and contact rarefaction are formed at the negative η-axis and positive ξ-axis, respectively. The delta shock $S_{\delta_{23}}$ meets the rarefaction wave R_{12} at point $A(2u_2, u_2 + u_3)$, and the curved delta shock continues toward point $B(0, \frac{u_3^2}{u_3 - u_2})$. Simultaneously, S_{ue} $(0 \le u \le u_3)$ and J_{e3} occur at B. The curved shock continues from B toward $C(2u_3, 2u_3)$. In addition, J_{e3} formed at point B ends at the singular point $D(u_3, u_3)$.

By contrast, J_{4d} meets S_{c4} at point $E(u_3 + u_4, u_4)$ and J_{ce} at the singular point D. Therefore, three contact discontinuities J_{e3}, J_{3c}, and J_{ce} meet at their singular point D. The shock $S_{ed}(= S_{c4})$ meets the rarefaction wave R_{d1} at point $F(u_3 + u_4, 2u_4)$, and the curved shock continues toward C. Both rarefaction waves R_{12} and R_{d1} meet at $(2u, 2u)$ for $u_3 \le u \le u_1$ between C and $G(2u_1, 2u_1)$. The solutions are shown in Figure 11. The initial condition is $u_1 = 0.56$, $u_2 = -0.15$, $u_3 = 0.43$, $u_4 = 0.21$.

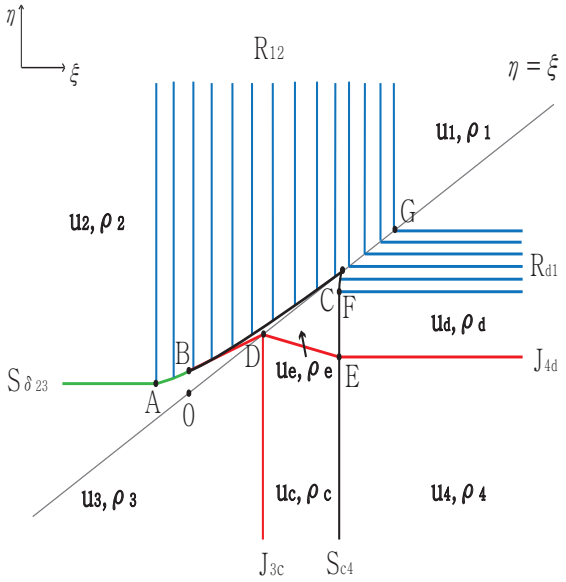

(**a**) Analytical solution

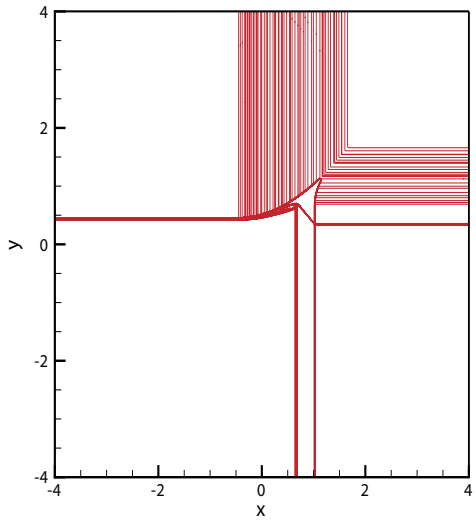

(**b**) Numerical solution

Figure 11. Case 11. $R + S_\delta + JS + JR$.

Case 12. $S_\delta + R + SJ + RJ \ \ (u_4 < u_1 < u_3 < 0 < u_2)$

From the initial discontinuity, a delta shock is formed at the positive η-axis and rarefaction is formed at the negative ξ-axis; in addition, shock-contact and rarefaction-contact are formed at the negative η-axis and positive ξ-axis, respectively. The straight delta shock $S_{\delta_{12}}$ meets R_{23}, and then a curved delta shock continues toward $A(\frac{u_1^2}{u_1-u_2}, 0)$. The new shock formed at A completely penetrates R_{23} and stops at the singular point $B(u_1+u_3, u_1+u_3)$. Moreover, J_{1e} formed at point A ends at the singular point $C(u_1, u_1)$. However, the shock S_{3c} completely penetrates the rarefaction wave R_{4d} from D to the point $E(\frac{u_1^2+u_3^2-2u_1u_4}{u_3-u_4}, 2u_1)$ and it stops at the singular point B. In addition, J_{c4} completely penetrates $R_{ce}(= R_{4d})$ from $F(u_4, 2u_4)$ to G and satisfies

$$\frac{d\eta}{d\xi} = \frac{\eta - u}{\xi - u}, \ \eta = 2u, \ \frac{\rho}{u} = \frac{\rho_4}{u_4}, \ u_4 \le u \le u_1. \tag{26}$$

which gives

$$\xi = \eta - \frac{\eta^2}{4u_4}, \quad 2u_4 \le \eta \le 2u_1. \tag{27}$$

The straight contact discontinuity J_{ed} continues from $G(\frac{2u_1u_4-u_1^2}{u_4}, 2u_1)$ to C, satisfying

$$\eta - u_1 = \frac{u_4}{u_4 - u_1}(\xi - u_1), \quad 2u_1 \le \eta \le u_1. \tag{28}$$

Here, J_{ed} meets J_{1e} and J_{d1} at their singular point C. The solutions are shown in Figure 12. The initial condition is $u_1 = -0.43$, $u_2 = 0.15$, $u_3 = -0.37$, $u_4 = -0.56$.

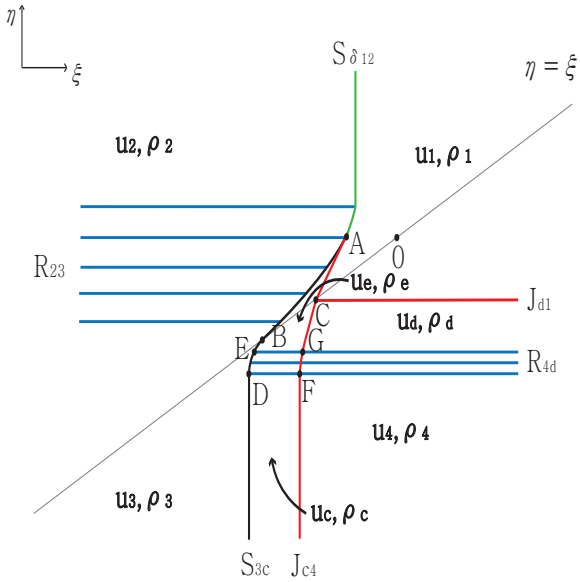

(**a**) Analytical solution

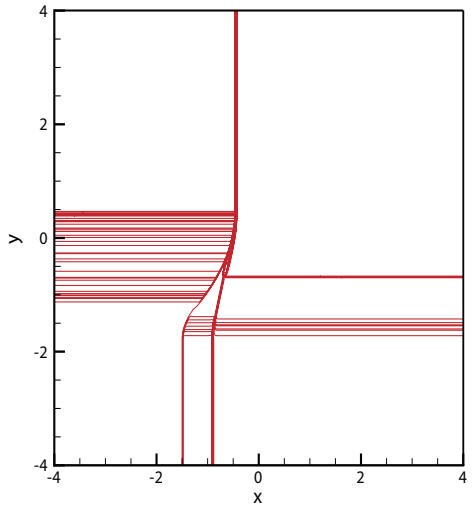

(**b**) Numerical solution

Figure 12. Case 12. $S_\delta + R + SJ + RJ$.

Case 13. $S_\delta + R + SJ + RJ \ \ (u_4 < u_3 < u_1 < 0 < u_2)$

In this case, the exterior waves at the initial discontinuity are exactly the same as those in case 12. The upper structures are also extremely similar to those in the previous case.

By contrast, both R_{23} and R_{4d} meet at $(2u, 2u)$ for $u_3 \leq u \leq u_1$ between $B(2u_1, 2u_1)$ and $D(2u_3, 2u_3)$. The shock S_{3c} meets R_{4d} at $(u_3 + u_4, 2u_4)$, and the curved shock then continues toward point D. Here, J_{c4} penetrates the entire rarefaction R_{4d} and the straight contact discontinuity continues from $(\frac{2u_1u_4 - u_1^2}{u_4}, 2u_1)$ to $C(u_1, u_1)$, which is a singular point of three contact discontinuities J_{1e}, J_{d1}, and J_{ed}. In case 12, the shock S_{3c} completely penetrates the rarefaction R_{4d}, but S_{3c} partially penetrates R_{4d} in case 13. This difference makes them topologically distinct. The solutions are shown in Figure 13. The initial condition is $u_1 = -0.37$, $u_2 = 0.15$, $u_3 = -0.43$, $u_4 = -0.56$.

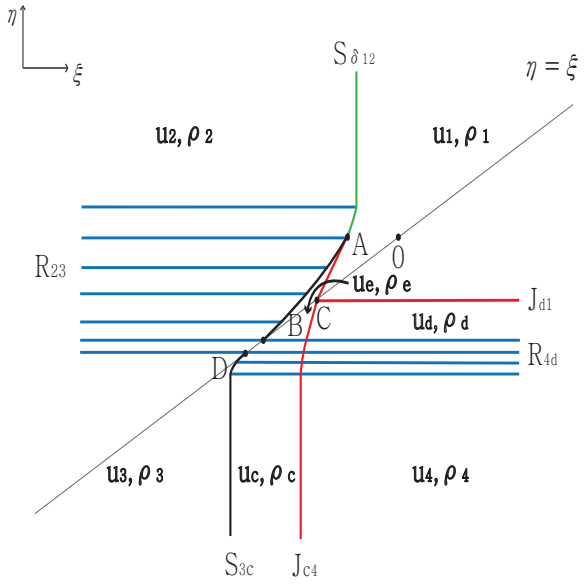

(**a**) Analytical solution

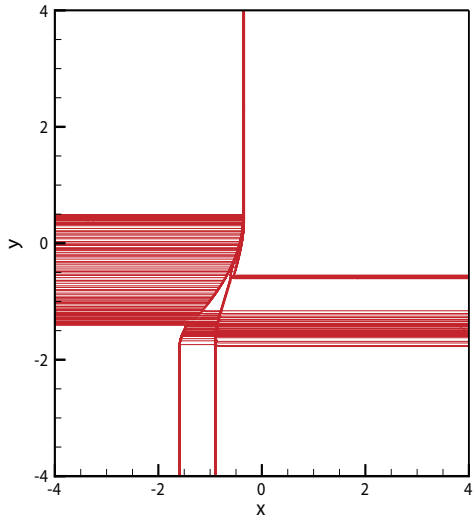

(**b**) Numerical solution

Figure 13. Case 13. $S_\delta + R + SJ + RJ$.

3.2.3. Two Shock Waves

$$\text{Case 14}: \begin{cases} JS + JS + R + S_\delta \ (12304), \ S_\delta + R + SJ + SJ \ (14302) \\ R + S_\delta + JS + JS \ (20143), \ SJ + SJ + S_\delta + R \ (40123) \end{cases}$$

Case 14. $JS + JS + R + S_\delta \ \ (u_1 < u_2 < u_3 < 0 < u_4)$

From the initial discontinuity, a contact shock is formed at the positive η-axis and negative ξ-axis, and rarefaction and delta shock are formed at the negative η-axis and positive ξ-axis, respectively. In addition, J_{2b} intersects with S_{a2} at point $P(u_1+u_2, u_2)$ and the new contact discontinuity J_{ae} occurs from P to $A(u_1, u_1)$. The shock $S_{a2}(=S_{eb})$ continues from P without changing the direction because $u_e = u_a$ and $u_b = u_2$. This shock S_{eb} meets the shock S_{b3} at the point $Q(u_1+u_2, u_2+u_3)$, and the new shock S_{e3} is formed at Q and ends at the singular point $H(u_1+u_3, u_1+u_3)$. By contrast, $S_{\delta_{41}}$ meets R_{34} at the point $R(2u_4, u_4+u_1)$, and the curved delta shock is then from R to $S(0, \frac{u_1^2}{u_1-u_4})$. Simultaneously, J_{e1} and S_{ue} $(u_3 \le u \le 0)$ are formed at S. The curved shock from S to T and the straight shock continues from the point $T(2u_3, \frac{u_1^2+u_3^2-2u_3u_4}{u_1-u_4})$ and meets S_{e3} at the singular point $H(u_1+u_3, u_1+u_3)$. However, the new contact discontinuity J_{e1} is from S to A and meets two contact discontinuities J_{1a} and J_{ae} at their singular point $A(u_1, u_1)$. The solutions are shown in Figure 14. The initial condition is $u_1 = -0.56$, $u_2 = -0.43$, $u_3 = -0.37$, $u_4 = 0.15$.

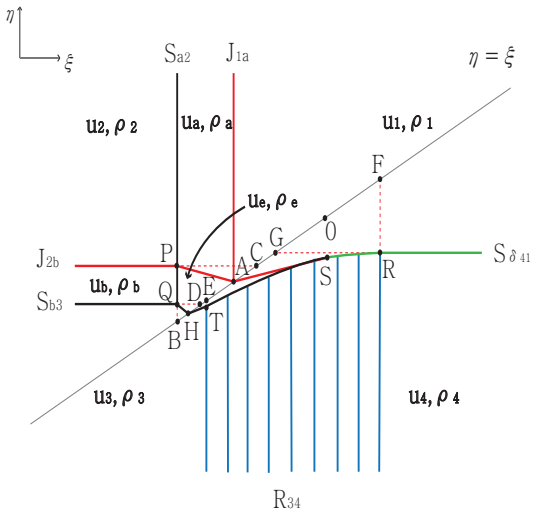

(**a**) Analytical solution

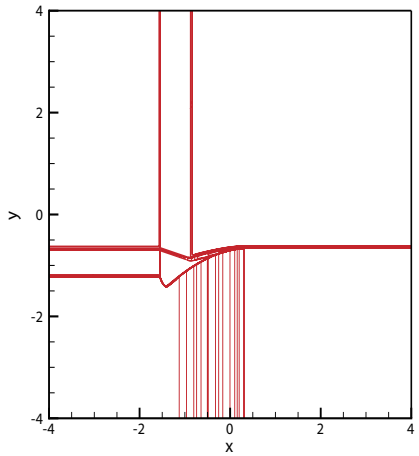

(**b**) Numerical solution

Figure 14. Case 14. $JS + JS + R + S_\delta$.

Author Contributions: Conceptualization, J.H. and W.H.; Formal anlysis, J.H., S.S. and M.S.; Funding Acquisition, J.H., S.S. and W.H.; Investigation, S.S. and M.S.; Methodology, S.S. and M.S.; Supervision,

W.H.; Writing−original dratf, J.H. and W.H.; Writing−review editing, J.H., S.S., M.S. and W.H. All authors have read and agreed to the published version of the manuscript.

Funding: This research was supported by a Basic Research Program through the National Research Foundation of Korea (NRF) funded by the Ministry of Education (Grant Nos. NRF-2018R1D1A1B0704 81 (W.H.), 2019R1I1A1A01057733 (J.H.), 2020R1I1A1A01056687 (S.S.)).

Acknowledgments: The authors thank the reviewers for constructive and valuable suggestions on the revision of this article.

Conflicts of Interest: The authors declare no conflict of interest.

References

1. Korchinski, D.J. Solutions of a Riemann Problem for a 2 × 2 System of Conservation Laws Possessing No Classical Weak Solutions. Ph.D. Thesis, Adelphi University, New York, NY, USA, 1977.
2. Zhang, T.; Zheng, Y.X. Conjecture on the structure of solutions of the Riemann problem for two-dimensional gas dynamics systems. *SIAM J. Math. Anal.* **1990**, *21*, 593–630. [CrossRef]
3. Tan, D.C.; Zhang, T. Two-dimensional Riemann problem for a hyperbolic system of nonlinear conservation laws: I. four-J cases. *J. Differ. Equ.* **1994**, *111*, 203–254. [CrossRef]
4. Tan, D.C.; Zhang, T. Two-dimensional Riemann problem for a hyperbolic system of nonlinear conservation laws: II. Initial data involving some rarefaction waves. *J. Differ. Equ.* **1994**, *111*, 255–282. [CrossRef]
5. Tan, D.C.; Zhang, T.; Chang, T.; Zheng, Y. Delta-shock waves as limits of vanishing viscosity for hyperbolic systems of conservation laws. *J. Differ. Equ.* **1994**, *112*, 1–32. [CrossRef]
6. Pang, Y.; Tian, J.P.; Yang, H. Two-dimensional Riemann problem for a hyperbolic system of conservation laws in three pieces. *Appl. Math. Comput.* **2012**, *219*, 1695–1711. [CrossRef]
7. Pang, Y.; Tian, J.P.; Yang, H. Two-dimensional Riemann problem involving three J's for a hyperbolic system of nonlinear conservation laws. *Appl. Math. Comput.* **2013**, *219*, 4614–4624. [CrossRef]
8. Shen, C. Riemann problem for a two-dimensional quasilinear hyperbolic system. *Electron. J. Differ. Equ.* **2015**, *2015*, 1–13.
9. Zhang, P.; Li, J.; Zhang, T. On two-dimensional Riemann problem for pressure-gradient equations of the Euler system. *Discret. Contin. Dyn. Syst.* **1998**, *4*, 609–634. [CrossRef]
10. Shen, C.; Sun, M. The Riemann problem for the pressure-gradient system in three pieces. *Appl. Math. Lett.* **2009**, *22*, 453–458. [CrossRef]
11. Sheng, W.; Zhang, T. *The Riemann Problem for the Transportation Equations in Gas Dynamics*; American Mathematical Soc.: Providence, RI, USA, 1999; Volume 654.
12. Cheng, H.; Liu, W.; Yang, H. Two-dimensional Riemann problems for zero-pressure gas dynamics with three constant states. *J. Math. Anal. Appl.* **2008**, *343*, 127–140. [CrossRef]
13. Wang, G.; Chen, B.; Hu, Y. The two-dimensional Riemann problem for Chaplygin gas dynamics with three constant states. *J. Math. Anal. Appl.* **2012**, *393*, 544–562. [CrossRef]
14. Chen, T.; Qu, A. Two-dimensional Riemann problem for Chaplygin gas dynamics in four pieces. *J. Math. Anal. Appl.* **2017**, *448*, 580–597. [CrossRef]
15. Shearer, M. The Riemann problem for 2 × 2 systems of hyperbolic conservation laws with case I quadratic nonlinearities. *J. Differ. Equations* **1989**, *80*, 343–363. [CrossRef]
16. Andrianov, N.; Warnecke, G. On the solution to the Riemann problem for the compressible duct flow. *SIAM J. Appl. Math.* **2004**, *64*, 878–901.
17. Yang, H. Generalized plane delta-shock waves for n-dimensional zero-pressure gas dynamics. *J. Math. Anal. Appl.* **2001**, *260*, 18–35. [CrossRef]
18. Hwang, W.; Lindquist, W.B. The 2-dimensional Riemann problem for a 2 × 2 hyperbolic conservation law I. Isotropic media. *SIAM J. Math. Anal.* **2002**, *34*, 341–358. [CrossRef]
19. Hwang, W.; Lindquist, W.B. The 2-dimensional Riemann problem for a 2 × 2 hyperbolic conservation law II. Anisotropic media. *SIAM J. Math. Anal.* **2002**, *34*, 359–384. [CrossRef]
20. Isaacson, E.L. *Global solution of a Riemann Problem for a Non-Strictly Hyperbolic System of Conservation Laws Arising in Enhanced Oil Recovery*; Enhanced Oil Recovery Institute, University of Wyoming: Laramie, WY, USA, 1989.
21. Keyfitz, B.L.; Kranzer, H.C. A system of non-strictly hyperbolic conservation laws arising in elasticity theory. *Arch. Ration. Mech. Anal.* **1980**, *72*, 219–241. [CrossRef]
22. Temple, B. Global solution of the Cauchy problem for a class of 2 × 2 nonstrictly hyperbolic conservation laws. *Adv. Appl. Math.* **1982**, *3*, 335–375. [CrossRef]
23. Sun, M. Construction of the 2D Riemann solutions for a nonstrictly hyperbolic conservation law. *Bull. Korean Math. Soc.* **2013**, *50*, 201–216. [CrossRef]
24. Shen, C.; Sun, M.; Wang, Z. Global structure of Riemann solutions to a system of two-dimensional hyperbolic conservation laws. *Nonlinear Anal.* **2011**, *74*, 4754–4770. [CrossRef]

25. Li, S.; Shen, C. Measure-Valued Solutions to a Non-Strictly Hyperbolic System with Delta-Type Riemann Initial Data. *Int. J. Nonlinear Sci. Numer. Simul.* **2020**, *21*, 1. [CrossRef]
26. Hwang, J.; Shin, M.; Shin, S.; Hwang, W. Two dimensional Riemann problem for a 2×2 system of hyperbolic conservation laws involving three constant states. *Appl. Math. Comput.* **2018**, *321*, 49–62. [CrossRef]
27. Keyfitz, B.L.; Kranzer, H.C. Spaces of weighted measures for conservation laws with singular shock solutions. *J. Differ. Equ.* **1995**, *118*, 420–451. [CrossRef]
28. Li, J.; Zhang, T.; Yang, S. *The Two-Dimensional Riemann Problem in Gas Dynamics*; Longman; Chapman and Hall/CRC: Boca Raton, FL, USA, 1998; Volume 98.
29. Kurganov, A.; Lin, C.T. On the reduction of numerical dissipation in central-upwind schemes. *Commun. Comput. Phys.* **2007**, *2*, 141–163.
30. Shin, M.; Shin, S.; Hwang, W. A treatment of contact discontinuity for central upwind scheme by changing flux functions. *J. Korean Soc. Ind. Appl. Math.* **2013**, *17*, 29–45. [CrossRef]